ELSEVIER

Mapping from ASTER stereo image data: DEM validation and accuracy assessment

Akira Hirano[a,*], Roy Welch[a], Harold Lang[b,1]

[a] *Center for Remote Sensing and Mapping Science (CRMS), Department of Geography, The University of Georgia, Athens, GA 30602, USA*
[b] *76-338 Wana Street, Kailua-Kona, Hawaii 96740, USA*

Abstract

The Advanced Spaceborne Thermal Emission and Reflection Radiometer (ASTER) on-board the National Aeronautics and Space Administration's (NASA's) Terra spacecraft provides along-track digital stereo image data at 15-m resolution. As part of ASTER digital elevation model (DEM) accuracy evaluation efforts by the US/Japan ASTER Science Team, stereo image data for four study sites around the world have been employed to validate prelaunch estimates of heighting accuracy. Automated stereocorrelation procedures were implemented using the Desktop Mapping System (DMS) software on a personal computer to derive DEMs with 30- to 150-m postings. Results indicate that a root-mean-square error (RMSE) in elevation between ± 7 and ± 15 m can be achieved with ASTER stereo image data of good quality. An evaluation of an ASTER DEM data product produced at the US Geological Survey (USGS) EROS Data Center (EDC) yielded an RMSE of ± 8.6 m. Overall, the ability to extract elevations from ASTER stereopairs using stereocorrelation techniques meets expectations.
© 2003 Elsevier Science B.V. All rights reserved.

Keywords: ASTER; DEM; stereocorrelation; validation

1. Introduction

All disciplines of scientific research involving studies of the earth's land surface require topographic data such as elevation, slope and aspect (Topographic Science Working Group, 1988; Bolstad and Stowe, 1994). Beginning more than 25 years ago, efforts have been directed toward developing satellites and sensor systems capable of producing global elevation data in digital formats (Ducher, 1980; Welch and Marko, 1981; Colvocoresses, 1982; Welch, 1985). The most successful of these efforts to date has been France's SPOT satellites (1–4), which beginning in 1986 with the launch of SPOT-1 have provided cross-track stereo images of 10- and 20-m resolution. Digital elevation models (DEMs) produced from these images by automated stereocorrelation are reported to be accurate between ± 5 and ± 20 m (i.e., root-mean-square error [RMSE] in the Z-coordinates) depending on the

* Corresponding author. Current address: Institute of History and Anthropology, University of Tsukuba, 1-1-1 Tennodai, Tsukuba, Ibaraki 305-8571, Japan. Tel.: +81-298-53-6589; fax: +81-298-53-4432.

E-mail address: ahirano@sakura.cc.tsukuba.ac.jp (A. Hirano).

[1] Associated with Jet Propulsion Laboratory, California Institute of Technology, Pasadena, CA, USA at the time the study was completed.

base-to-height (B/H) ratio (Welch, 1990; Al-Rousan and Petrie, 1998). However, the cost and difficulty of obtaining cloud-free, cross-track SPOT stereo coverage for many areas of the world has limited the possibilities for producing DEMs of large, contiguous areas. Consequently, attention has turned to other sensor configurations, including an along-track stereo sensor system to be incorporated in the SPOT-5 satellite scheduled for launch in April 2002 (SPOT Image, 2001).

In military circles, it is anticipated that a global DEM of the land area of the earth produced from the Shuttle Radar Topography Mission (SRTM) data recorded in February 2000 and accurate to approximately ± 16 m will be completed by 2003 (Farr et al., 2000). Meanwhile, in the civilian community, the focus is on stereo image data recorded in the along-track direction by the Advanced Spaceborne Thermal Emission and Reflection Radiometer (ASTER) on-board the National Aeronautics and Space Administration's (NASA's) Terra satellite that was launched in December 1999 (Yamaguchi et al., 1998). This paper will discuss ASTER and the methods being used to derive and validate DEMs produced from ASTER stereo image data. Consideration is also given to the utility of the ASTER DEMs for various mapping applications.

2. The ASTER sensor stereo system for DEM generation

The ASTER sensor is designed to provide image data in 14 visible, near-infrared, short wavelength infrared and thermal infrared spectral bands (Table 1). Stereo image data are recorded only in Band 3, which is the near-infrared wavelength region from 0.78 to 0.86 μm, using both nadir and aft-looking telescopes. From the nominal Terra altitude of 705 km, the "pushbroom" linear array sensor covers a 60-km-wide ground track at a 15-m spatial resolution. As shown in Fig. 1, there is an approximately 60-s interval between the time the nadir telescope passes over a ground location and the aft telescope records the same location on the ground track of the satellite. Images generated from the nadir and aft telescopes yield a B/H ratio of 0.6, which is close to ideal for generating DEMs by automated techniques for a

Table 1
Technical specifications of ASTER sensor and Terra satellite orbital parameters

Technical specifications	Terra ASTER stereo
Bands in visible/near-infrared	3
Bands in short wavelength infrared	5
Bands in thermal infrared	6
Stereo capability	Yes
	Bands 3N and 3B (nadir and aft-looking telescopes)
	0.78–0.86 μm
Stereo imaging geometry	Along-track
Base-to-height (B/H) ratio	0.6
Pixel size	15 m
Scene coverage	60 km × 60 km
Orbital path	Near-polar sun-synchronous
Orbital altitude	705 km
Orbital inclination	98.2°
Repeat cycle	16 days

variety of terrain conditions. A major advantage of the along-track mode of data acquisition (as compared to cross-track) is that the images forming the stereo-pairs are acquired a few seconds (rather than days) apart under uniform environmental and lighting conditions, resulting in stereopairs of consistent quality that are well suited for DEM generation by automated stereocorrelation techniques (Colvocoresses, 1982; Fujisada, 1994).

The ASTER sensor has been acquiring science data in an operational mode since March 2000. This paper examines the possibilities of creating DEMs using test areas at four locations: (1) Mt. Fuji, Japan; (2) Andes Mountains, Chile–Bolivia; (3) San Bernardino, CA; and (4) Huntsville, AL (Fig. 2).

3. Study areas and datasets

The characteristics of each of the study areas and their corresponding ASTER datasets are discussed below (see Fig. 3).

3.1. Mt. Fuji

The Mt. Fuji (3776 m) study area (35°28′ N, 139°04′ E) is located approximately 100 km west of Tokyo, Japan (Fig. 3a). Terrain ranges from relatively
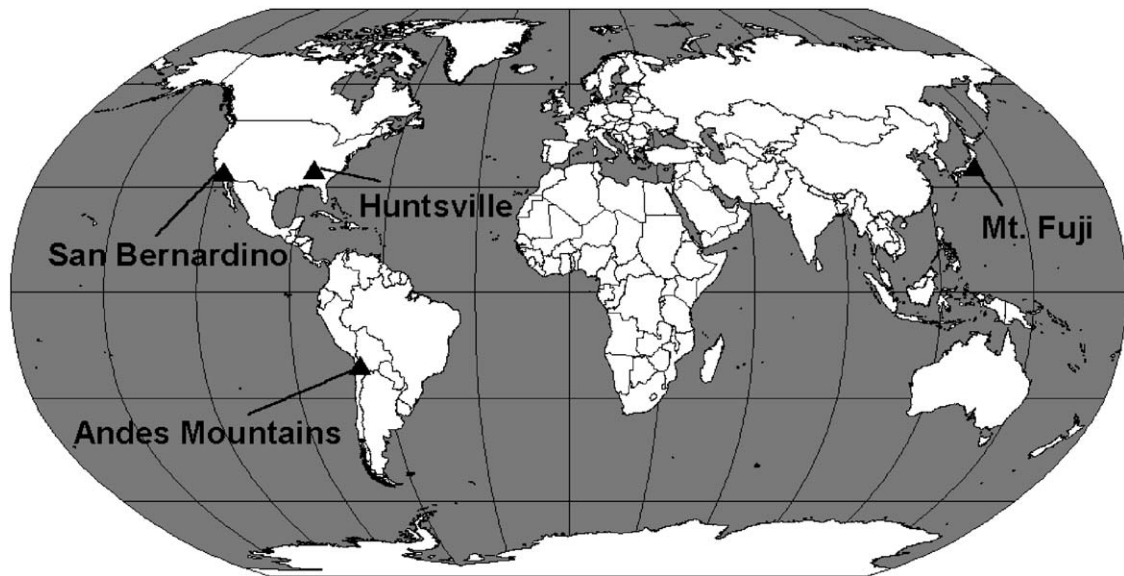
Fig. 1. Simplified diagram of the imaging geometry for ASTER along-track stereo.

low and flat rice fields at the base of the mountain (~ 220 m) to steep lava slopes extending to the top of Mt. Fuji which is just outside the boundaries of the study area. Total relief is about 2100 m for the area of study.

Images for the Mt. Fuji study area included a 4100 pixel × 8893 line (62 × 113 km) ASTER stereopair recorded in May 2000. This stereopair was processed prior to the formal release of standard Level 1A data (radiometric and geometric coefficients attached, but not applied). Sixteen 1:25,000-scale topographic maps (contour interval = 10 m) produced by Geographical Survey Institute (GSI) in Japan yielded a total of 50 ground control points (GCPs) and 331 check points. The expected accuracy of these digitized points is estimated to be approximately ± 5 m in both planimetric position and elevation.

3.2. Andes mountains

The Andes mountains study area (21°00′ S, 68°13′ W) is located along the Chile–Bolivia border and is dominated by the Pampa Luxsar lava complex (Fig. 3b). Rugged terrain is featured with elevations ranging from relatively low, flat lava flow areas at approximately 3500 m to several high cone-shaped volcanoes including Cerro Luxsar, Olca and Paruma reaching elevations of approximately 5700 m. Total relief is about 2200 m.

An ASTER stereopair (Level 1A) of 4980 pixels × 4200 lines (75 × 63 km) recorded on April 7, 2000 was provided for evaluation. Eleven 1:50,000-scale topographic maps (contour interval = 20 m) produced by the Instituto Geográfico Militar of Bolivia were employed to select 18 GCPs and 46 check points.

Fig. 2. Study area location map.

The coordinates of these points were digitized from the topographic maps. The accuracy of these points in planimetric position and elevation is estimated to be approximately ± 10 m.

3.3. San Bernardino

The San Bernardino, CA (pop. 185,401) study area (34°14′ N, 117°20′ W) is located just east of Los Angeles and is on the edge of the Coast Ranges (Fig. 3c). This is a densely populated region that features both urban and rural land use. Elevations range from approximately 200 m for the flat urban areas to over 1700 m in the high mountains to the north and east, providing a total relief in excess of 1500 m.

The ASTER image dataset for this study area is a 4100 pixel × 4200 line (62 × 63 km) Level 1A stereopair recorded on October 8, 2000. Nine US Geological Survey (USGS) 1:24,000-scale topographic quadrangles (contour interval = 10–40 ft or 3–12 m) cover the study area. Some 17 GCPs were collected by Dr. Michael Abrams of the Jet Propulsion Laboratory (JPL) using a Trimble™ Pathfinder® Pro XRS Differential Global Positioning System (DGPS) unit. Over 100 check points (expected positional and elevation accuracy of approximately ± 5 m) were digi-

tized by the authors from the topographic maps. Additionally, two USGS 7.5-min Level 2 DEMs (for Silverwood Lake and San Bernardino North quadrangles) with a vertical accuracy of about ± 6 m provided the reference elevations for the ASTER DEM accuracy assessment.

3.4. Huntsville

The Huntsville, Alabama (pop. 158,216) study area (34°49′ N, 86°42′ W) is located at the foot of the Appalachian Mountains in northeast Alabama (Fig. 3d). Terrain is flat to rolling in the urban and residential areas surrounded by forest and agricultural land (~ 180 m) with high hills to the east of the city rising up to approximately 500 m. Total relief is about 300 m.

A Level 1A ASTER stereopair of 4100 pixels × 4200 lines (62 × 63 km) recorded on July 1, 2000 is the dataset acquired for evaluation. Thirteen USGS 1:24,000-scale topographic quadrangles (contour interval = 10–20 ft or 3–6 m) cover the study area. These topographic maps were supplemented by a USGS 7.5-min Level 2 DEM of Huntsville with a reported vertical accuracy of 1.5 m (one half of the contour interval of the corresponding USGS 1:24,000-scale topographic quadrangle).
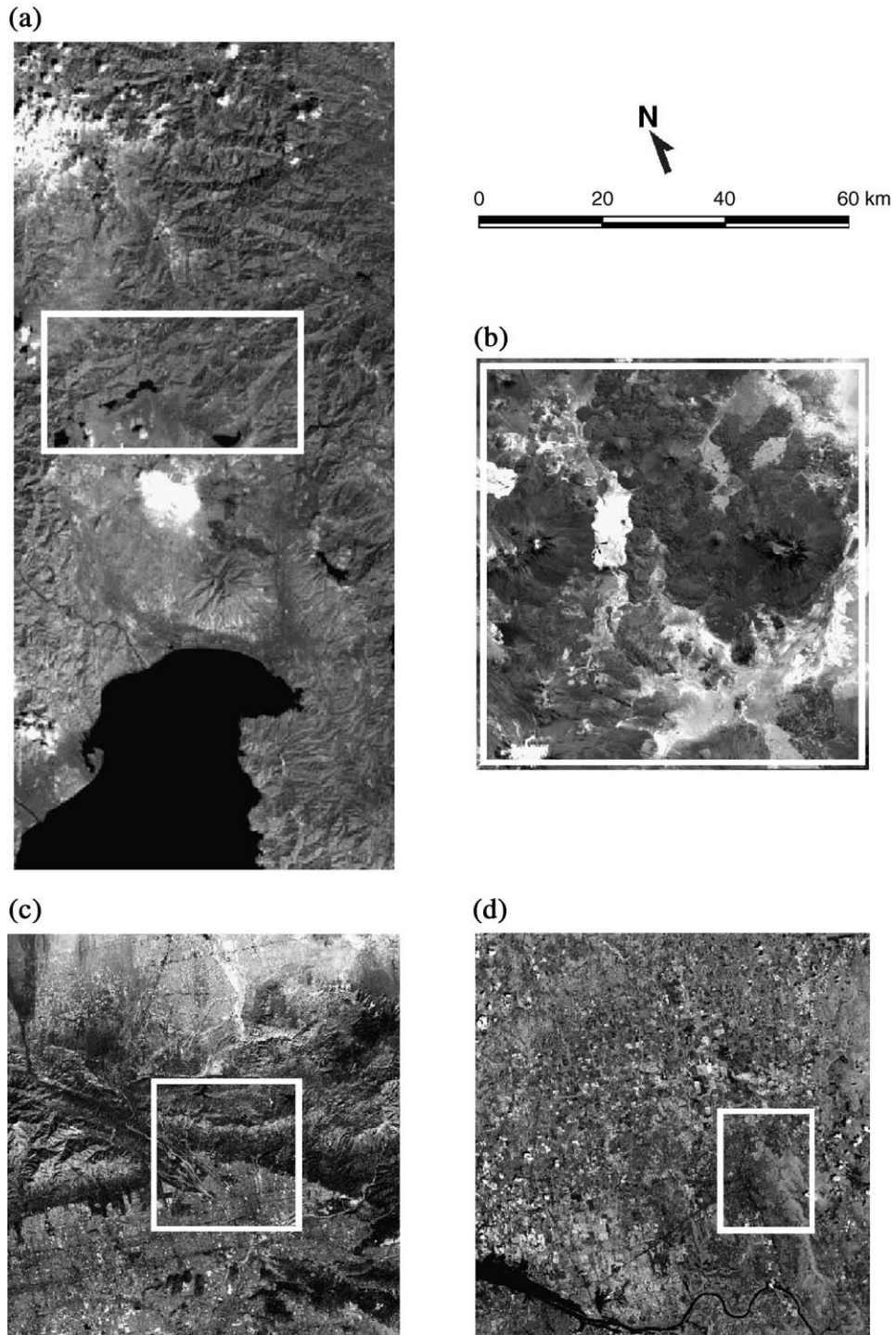
Fig. 3. ASTER band 3 (nadir) images of the study areas. (a) Mt. Fuji, Japan, (b) Andes Mountains, Chile–Bolivia, (c) San Bernardino, CA and (d) Huntsville, AL. White boundaries shown in the images represent the stereopair coverage.

Table 2
Eleven ASTER DEM validation sites selected by the members of the ASTER Science Team DEM working group to assess the quality of ASTER DEM data products (listed in priority order) (Welch et al., 1998)

Site	Approximate longitude/latitude
Mt. Kiso-Komagatake, Japan	36°N/138°E
Huntsville, AL, USA	35°N/87°W
Mt. Fuji, Japan	33°N/130°E
Taxco/Iguala, Mexico	18°N/99°W
Mt. Tsukuba, Japan	36°N/140°E
Drum Mountains, UT, USA	40°N/113°W
Mt. Aso, Japan	33°N/131°E
Mt. Etna, Italy	38°N/15°E
Mt. Unzen, Japan	33°N/130°E
Saga Plain, Japan	33°N/130°E
Lake Okoboji, IA, USA	43°N/96°W

Huntsville is one of eleven validation sites designated by the US/Japan ASTER Science Team DEM Working Group (Table 2). Consequently, this is our primary study area and a DGPS control survey was performed using a Trimble Pathfinder Pro DGPS unit with OMNISTAR real-time corrections in December 1999. Forty-three well-distributed GCPs were surveyed to control the ASTER stereopairs and to assess the accuracy of the ASTER DEM. In addition, 512 DGPS points were collected from a moving survey vehicle.

4. DEM generation by stereocorrelation

Automated stereocorrelation has become a standard method of generating DEMs from digital stereo images. Stereocorrelation is a computational and statistical procedure utilized to derive a DEM automatically from a stereopair of registered images (Ackermann, 1984; Ehlers and Welch, 1987; Lang and Welch, 1999). The core of stereocorrelation is automatic image matching. Although approaches may vary according to the software employed, the procedures normally include the collection of GCPs, determination of parallax values on a per pixel or per DEM post-basis using automatic image matching techniques and, finally, post-processing to remove anomalies from the DEMs (Kok et al., 1987). Two types of DEM products can be generated: (1) a relative DEM where the elevations are not tied to a ground or map datum; and (2)

an absolute DEM where the locations of the DEM posts are fitted to a standard map coordinate system and the elevations are referenced to sea level.

4.1. Design specifications and ASTER DEM production

The US/Japan ASTER Science Team DEM Working Group established the design specifications for ASTER DEM data products, as shown in Table 3. Both relative and absolute DEMs are created with compatible formats and elevation postings every 30 m (Lang et al., 1996; Fujisada, 1998). Relative DEMs, referenced to the lowest elevation in the scene, require no GCPs and are generated by using only the satellite ephemeris data (Fujisada et al., 2001). These relative DEMs are good to ± 10–30 m. They are produced at a rate of 30 scenes per day at the Science Data Processing Segment (SDPS) of the ASTER Ground Data System (GDS) in Japan using Level 1A data for input. The design specifications for absolute DEMs, based on prelaunch simulations, were established to have an accuracy between ± 7 and ± 50 m, depending on the

Table 3
Definitions/specifications for ASTER DEM data products (after Lang and Welch, 1999)

Unit of Coverage:	60 × 60 km ASTER scene		
Format:	Data consist of a regular array of elevations (in m) referenced to either the lowest elevation in the scene ("relative DEM") or the mean sea level ("absolute DEM") and projected in the Universal Transverse Mercator (UTM) coordinate system.		
Resolution:	(1) $X-Y$: 30 m (posting) (2) Z: 1 m (smallest increment)		

Product name	Number of GCPs (minimum)	GCP (RMSExyz) accuracy (m)	DEM (RMSExyz) accuracy (m)
Relative DEM	0	N/A	10–30[a]
Absolute DEM	1	15–30	15–50[b]
Absolute DEM	4	5–15	7–30[b]

[a] Z values referred to local vertical datum.
[b] Z values referred to absolute vertical datum (mean sea level).

Table 4
Summary of ASTER DEM generation and accuracy assessment for the study areas

Study area and DEM parameters	Image-to-image registration (pixel)	Image-to-ground registration		Completeness of stereocorrelation (percent success)	Number of check points (source)	RMSEz (m)
		Number of GCPs (source)	RMSExy (pixel)			
Mt. Fuji 1600 × 1400 pixels (24 × 21 km) 75 m posting	± 0.85	5 map points (1:25,000)	6 m (± 0.4)	97	51 map points (1:25,000)	± 26.3
Andes Mountains 3700 × 3800 pixels (55.5 × 57 km) 150 m posting	± 0.76	5 map points (1:50,000)	19.5 m (± 1.3)	99	53 map points (1:50,000)	± 15.8
San Bernardino 1500 × 1500 pixels (22.5 × 22.5 km) 75 m posting	± 1.13	12 DGPS points	18 m (± 1.2)	99	16 map points (1:24,000)	± 10.1
Huntsville 1500 × 1800 pixels (22.5 × 18 km) 30 m posting	± 0.62	8 DGPS points	9 m (± 0.6)	97	39 DGPS points	± 7.3
					512 DGPS points (kinematic)	± 11.1
					239,776 posts (USGS DEM)	± 14.7

number of GCPs provided (O'Neill and Dowman, 1993; Dowman and Neto, 1994; Giles and Franklin, 1996; Tokunaga et al., 1996). The USGS EROS Data Center (EDC) Distributed Active Archive Center (EDC DAAC) produces relative and absolute ASTER DEMs using Level 1A data for input at a nominal rate of one DEM per day, but current production rates are somewhat greater (Bailey, 2001, personal communication). Absolute DEMs require a minimum of eight evenly distributed GCPs to be supplied by the end-user requesting the generation of the DEM product. Ground control points are specified in the Universal Transverse Mercator (UTM) coordinate system, referenced to the World Geodetic System of 1984 (WGS 84) ellipsoid for foreign areas and to the North American Datum of 1983 (NAD 83) for areas within the United States and Canada (Snyder, 1987; Schwartz, 1989).

Procedures specified by the ASTER Science Team DEM Working Group for extracting Z-coordinates from the ASTER stereo image data were to use commercially available software such as PCI Geomatica™ OrthoEngine® (PCI Geomatics), Desktop
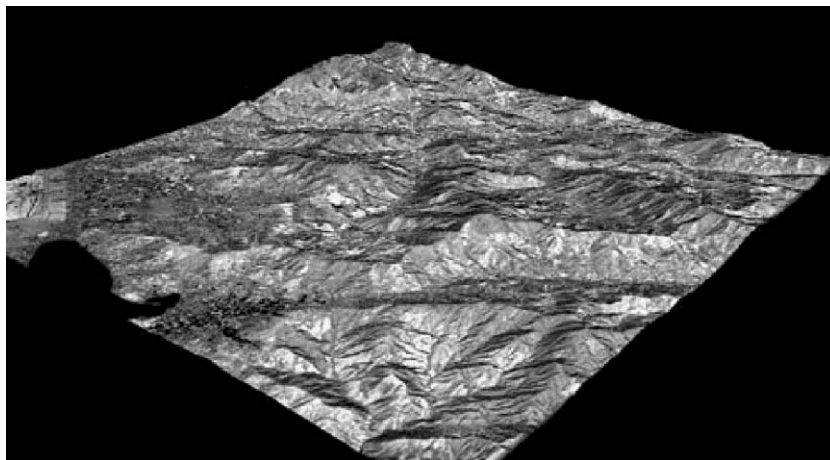

Fig. 4. 3D perspective view of ASTER DEM for the Mt. Fuji study area generated by using automated stereocorrelation techniques. DEM was draped by the ASTER band 3 (nadir) image. Mt. Fuji itself is not included in the stereopair coverage.
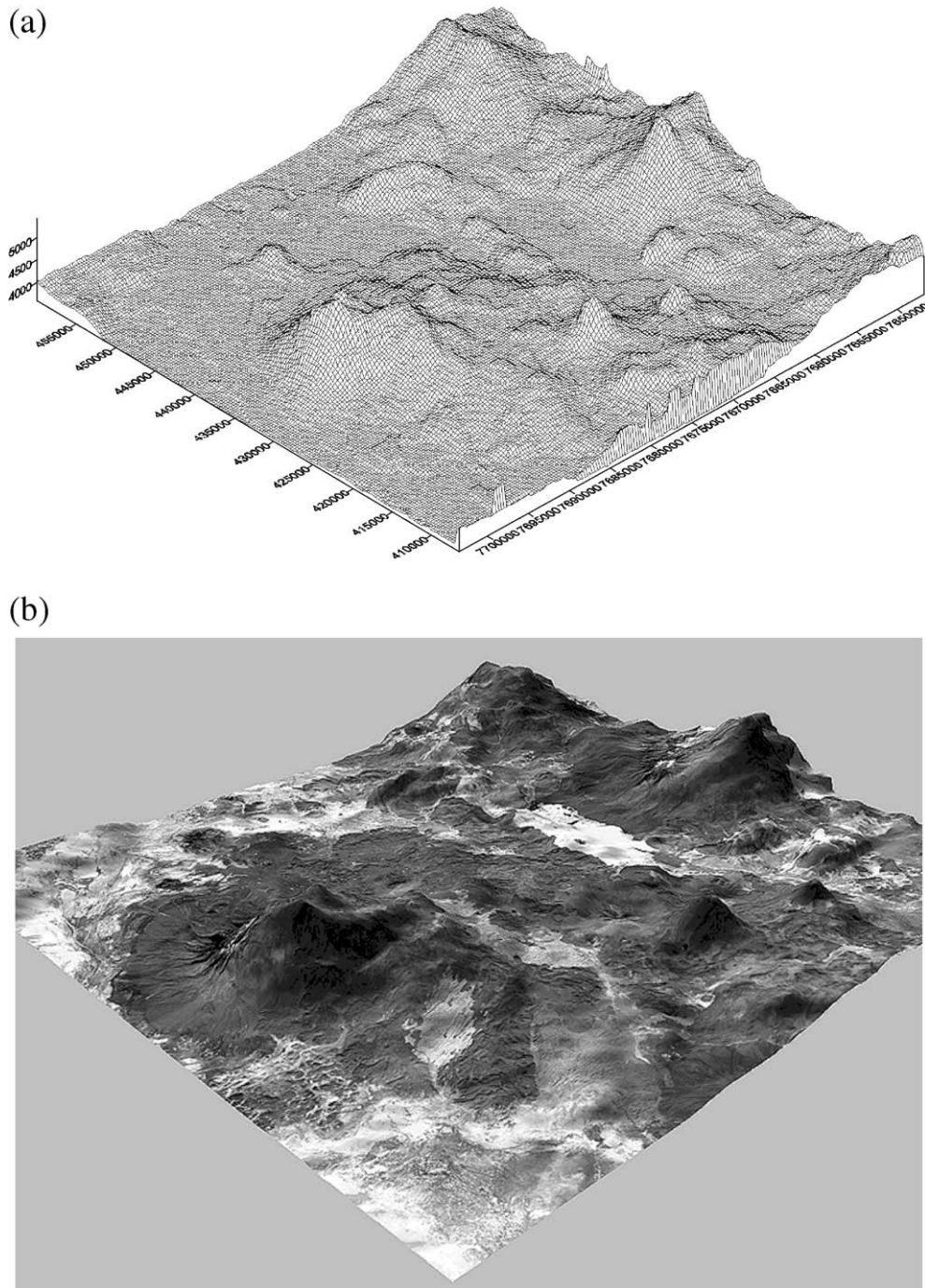
(a)

(b)

Fig. 5. (a) Wire-frame representation and (b) 3D perspective view of ASTER DEM for the Andes Mountain study area.

Mapping System (DMS)™ (*R-WEL*) and ERDAS Imagine® OrthoBASE Pro™ (ERDAS). The PCI software is employed at EDC for ASTER DEM production.

4.2. DEM generation with the DMS software

This study was conducted using the *R-WEL* DMS software operational on a standard Dell personal computers equipped with a Pentium Pro Processor (333 MHz) running under the Microsoft Windows® 95 operating system.

The ASTER stereo images for each study area were placed in register and fitted to the UTM coordinate system to within ±0.5 to ±1.0 pixel using GCPs clearly identifiable on both images of the stereopair (Table 4). As previously discussed, these GCPs were collected from topographic maps of the study areas and/or from DGPS surveys. Stereocorrelation was undertaken using correlation windows of 13×13 to 19×19 pixels and DEMs produced at post intervals of 30–150 m, depending on the study area. On average, with relatively large correlation windows, approximately 4000 elevation points per min were computed. The success of the correlation ranged from 97% to 99%, indicating that artifacts such as spikes and outliers in the DEMs were minimal. Any such outliers were removed by applying a median filter with kernel sizes of three to five. Perspective views were created by draping the images over the DEMs as shown in Figs. 4–6.
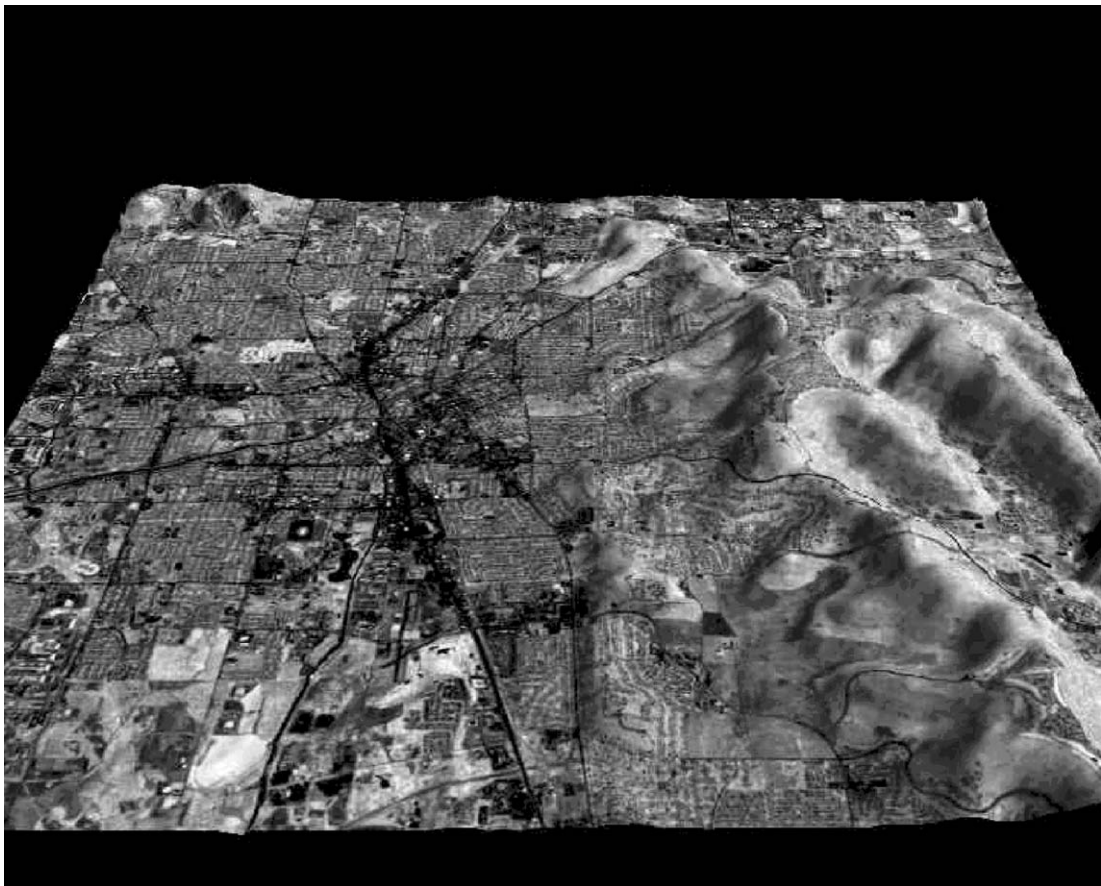
Fig. 6. 3D perspective view of the ASTER DEM for the Huntsville study area.

5. ASTER DEM accuracy assessment

The results of the stereocorrelation for each of the study areas are summarized in Table 4, along with the vertical accuracy determined by comparing the computed *Z*-coordinate values at check points with those collected from the topographic maps or DGPS surveys. Comparison at check points for the Mt. Fuji study area yielded a RMSEz of ± 26.3 m. Consider-

ing that the ASTER stereo images used to create the DEM were processed prior to the official release of Level 1A image data, this figure is quite favorable and falls within the design specification RMSEz of ± 7 to ± 50 m. The RMSEz for the remaining three study areas (Level 1A data) ranged from ± 7.3 to ± 15.8 m. In addition, for Huntsville study area, ASTER DEM produced with the DMS software was further assessed for vertical accuracy using previously dis-
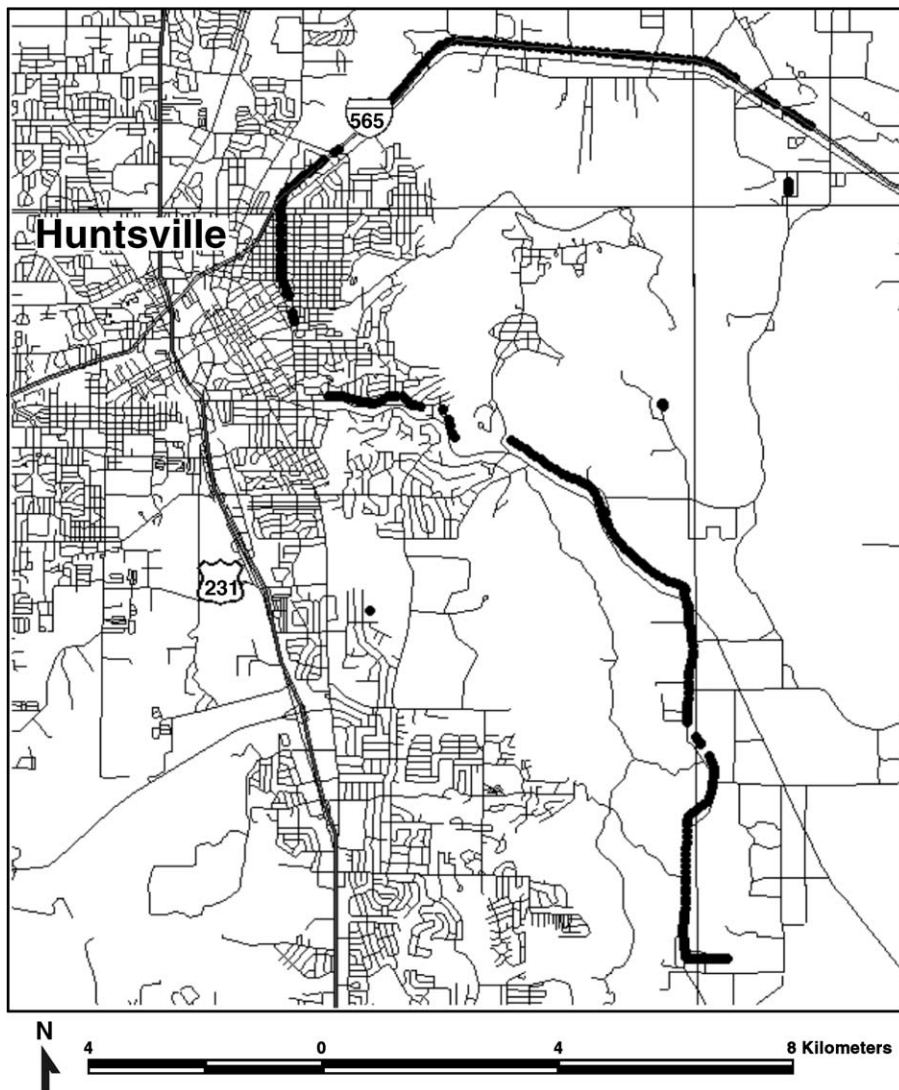
Fig. 7. Additional ASTER DEM elevation accuracy assessment. As many as 512 Differential Global Positioning System (DGPS) surveyed check points sequentially collected on a moving survey vehicle (solid black line) were used to check the DEM elevations. Check points are overlaid on top of the Huntsville USGS digital line graph (DLG). Root-mean-square error in Z (RMSEz) for this test resulted in ± 11.1 m.

cussed 512 kinetically collected DGPS survey points and resulted in the similar RMSEz of ± 11.1 m (Fig. 7). Additional error assessment for the Huntsville study area was accomplished by subtracting the ASTER Z values on a post-by-post basis from those on an USGS 7.5-min Level 2 DEM. The resulting RMSEz for this testing was ± 14.7 m when all differences were assumed to result from errors in the ASTER DEM (Fig. 8). In general, we were able to achieve a RMSEz of ± 7 to ± 15 m. This varied according to the study areas and reliability of the maps, but, overall, the height accuracy within range of design specifications were achieved.

Comparable transect elevations were plotted from the reference maps and DEMs, and from the computed ASTER DEMs to provide both a quantitative and visual assessment of ASTER DEM quality as shown in Fig. 9a–c. Despite a relatively high RMSEz in comparison with other study areas using Level 1A stereopairs, the elevation profiles developed for the Mt. Fuji study area showed good accordance in all elevation range. Elevation profiles also showed good agreement with the transects developed from the USGS 7.5-min Level 2 DEMs (reported accuracy of

± 6 m for San Bernardino and ± 3 m for Huntsville, respectively).

5.1. Validation of ASTER DEM produced by EDC

As previously discussed, 11 validation sites were selected by the US/Japan ASTER Science Team DEM Working Group to assess the quality of ASTER DEM products produced by distribution centers such as the USGS EDC in Sioux Falls, SD (Welch et al., 1998; Lang and Welch, 1999). These validation sites include the Huntsville study area. Consequently, EDC generated a DEM for an entire ASTER stereopair acquired on July 1, 2000 of the Huntsville site using the PCI Geomatica OrthoEngine software (PCI Geomatics) and 35 GCPs supplied by the authors (SC:AST_L1A.001:2001237385). This DEM has a 30-m post spacing totaling approximately 6,000,000 elevation points (Fig. 10). On the whole, the DEM appears to be satisfactory, although areas that could not be correlated due to clouds or cloud shadows appear as black artifacts.

The vertical accuracy of this ASTER DEM was checked against 40 DGPS survey points and 12 points

Histogram of Elevation Differences
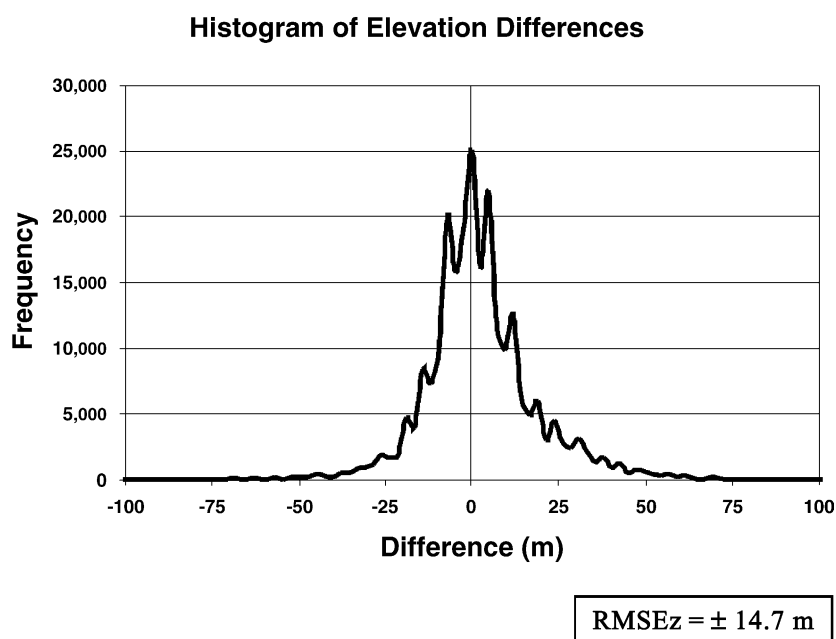

RMSEz = ± 14.7 m

Fig. 8. Histogram of elevation differences between USGS 7.5-m Level 2 DEM (reported RMSEz ± 3 m) covering the Huntsville, AL quadrangle and the corresponding ASTER DEM.
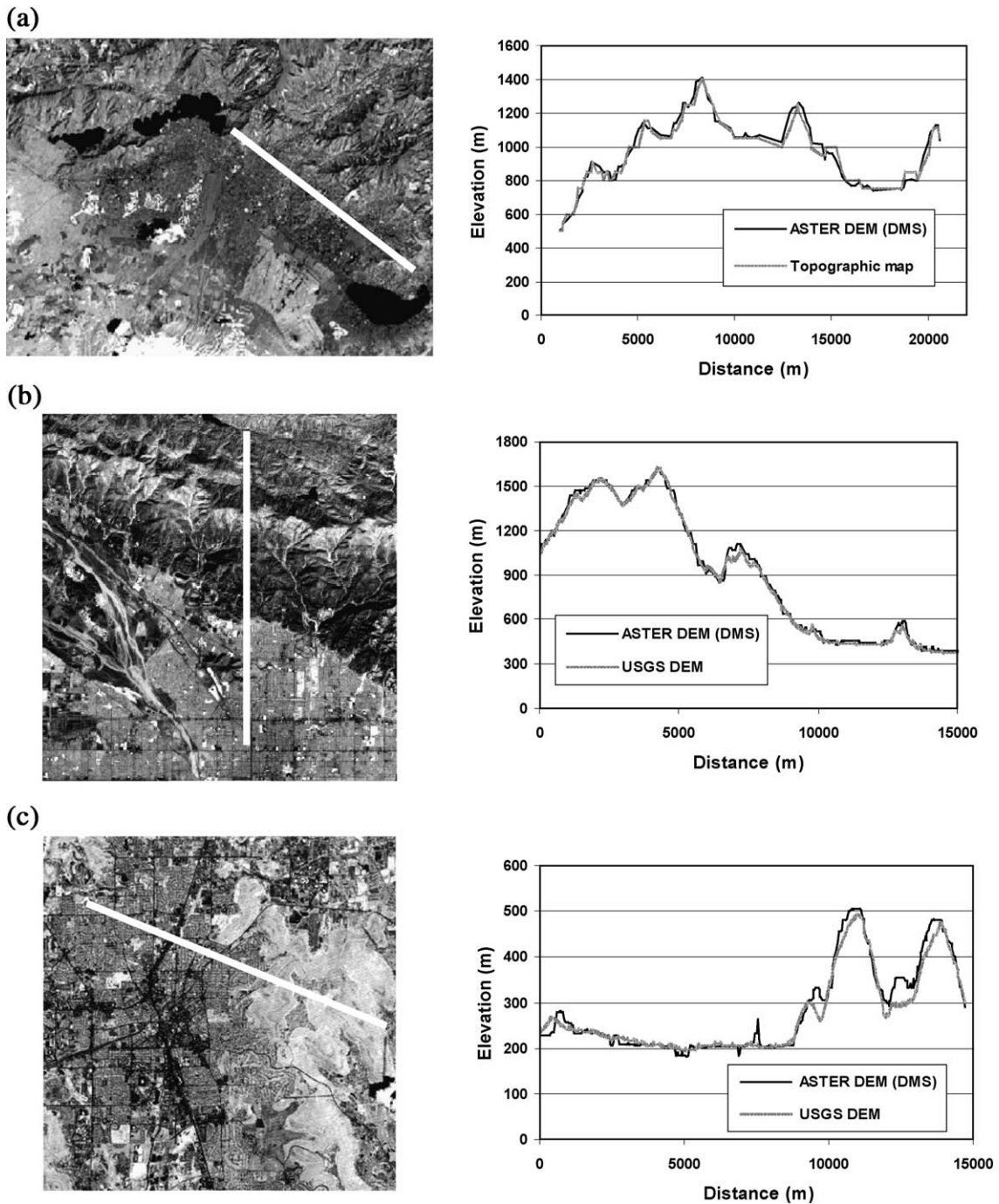
Fig. 9. Profile comparisons between ASTER DEM elevations and reference maps and DEMs. White lines shown in the images are transects used for plotting elevation profiles. Reference elevations for the Mt. Fuji study area (a) were digitized from a series of 1:25,000-scale topographic maps. USGS 7.5-min Level 2 DEM elevations for a portion of the San Bernardino (b) and Huntsville (c) study areas were plotted against the ASTER DEM elevations generated with the DMS™ software (*R-WEL*) package using stereocorrelation techniques.
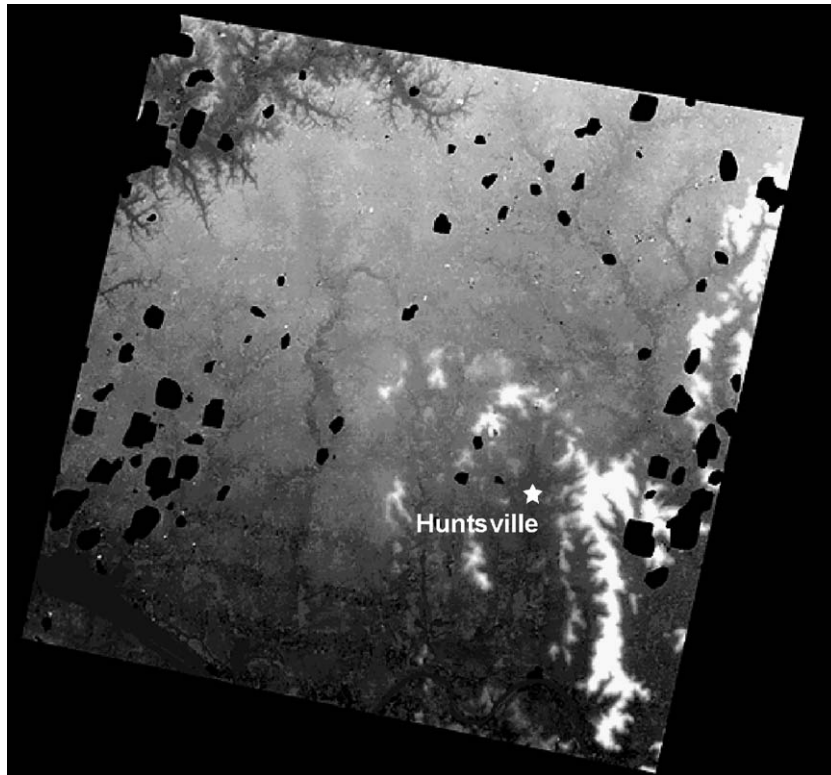
Fig. 10. ASTER DEM produced by the EROS Data Center (EDC) for the entire Huntsville ASTER scene of approximately 60×60 km. Elevations are coded in shades of gray, ranging from dark (low) to light (high elevation). Artifacts found in the DEM correspond with areas of clouds and cloud shadows, which could not be correlated.

digitized from USGS 1:24,000-scale topographic quadrangles, yielding an RMSEz of ± 8.6 m. This generally corresponds with other validation results reported by EDC (EDC DAAC, 2001).

An elevation transect was developed to further compare the ASTER DEM produced by EDC with a USGS Level 2 DEM (Fig. 11). At the lower elevations, transects from the ASTER DEM agree with
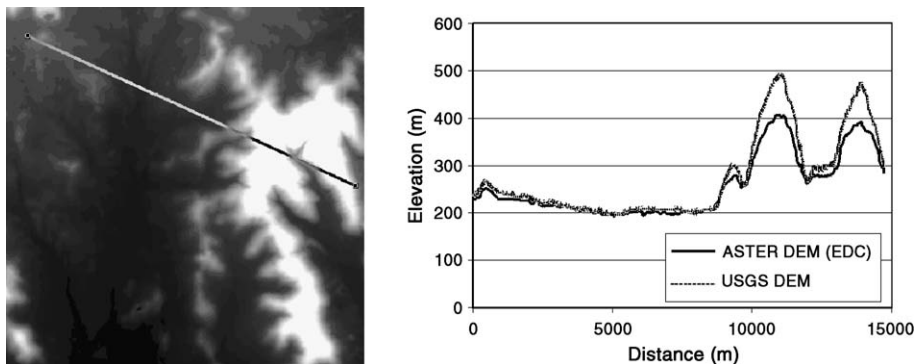
Fig. 11. Profile comparison between ASTER DEM elevations and USGS 7.5-min Level 2 DEM elevations for a portion of the Huntsville, AL quadrangle. The ASTER DEM was generated by the EROS Data Center (EDC).

those from the USGS DEM. However, the magnitude of difference become greater as terrain elevation increases. This problem also has been noted by EDC.

6. Conclusion

The Advanced Spaceborne Thermal Emission and Reflection Radiometer (ASTER) on-board NASA's satellite Terra is a high-resolution multispectral sensor that provides along-track stereo image data of the earth in the near-infrared wavelength region at a base-to-height (B/H) ratio of 0.6. With 15-m resolution, the along-track stereo images are well suited for generating DEMs by automated stereocorrelation techniques.

Evaluations of vertical accuracy resulting from stereocorrelation indicate that RMSEz values of approximately ± 7 to ± 15 m can be expected when using software such as the PCI Geomatica OrthoEngine and *R-WEL*, DMS packages with images of good quality and adequate ground control. Overall, correlation success rate ranging from 97% to 99% is achieved for images of study areas in Japan, South America and the United States. Validation of an official ASTER DEM data product generated by EDC using 35 GCPs provided by the authors was also carried out for the Huntsville, AL study area. A comparison of the ASTER DEM elevations against 52 reference elevations produced an RMSEz of ± 8.6 m. Overall, the ability to extract elevations from ASTER stereopairs using stereocorrelation techniques meets expectations.

Based on the results obtained in this study, it appears that ASTER stereo images will prove suitable for a range of environmental mapping tasks involving the use of DEMs. Examples of such tasks include landform studies, mapping of glaciers, assessment of volcanic activity and comparative terrain visualization studies requiring the computer generation of 3D perspective views from the stereo images. The ASTER data should also prove suitable for topographic mapping of high relief areas at scales of 1:50,000 to 1:100,000 with contour intervals of 40 m or larger. As necessary, ASTER DEMs also can be used to correct for relief displacements in images produced by other satellites and to provide the basis for orthoimage development from both aircraft and satellite image data.

References

Ackermann, F., 1984. Digital image correlation: performance and potential application in photogrammetry. Photogrammetric Record 11 (64), 429–439.

Al-Rousan, N., Petrie, G., 1998. System calibration, geometric accuracy testing and validation of DEM and orthoimage data extracted from SPOT stereopairs using commercially available image processing systems. International Archives of Photogrammetry and Remote Sensing 32 (4), 8–15.

Bolstad, P.V., Stowe, T., 1994. An evaluation of DEM accuracy: elevation, slope, and aspect. Photogrammetric Engineering and Remote Sensing 60 (11), 1327–1332.

Colvocoresses, A.P., 1982. An automated mapping satellite system (Mapsat). Photogrammetric Engineering and Remote Sensing 48 (10), 1585–1591.

Dowman, I., Neto, F., 1994. The accuracy of along track stereoscopic data for mapping: results from simulations and JERS OPS. International Archives of Photogrammetry and Remote Sensing 30 (4), 216–221.

Ducher, G., 1980. Cartographic possibilities of the SPOT and spacelab projects. Photogrammetric Record 10 (56), 167–180.

EDC DAAC, 2001. ASTER DEM data product. URL: http://edcdaac.usgs.gov/aster/ast14dem.html (accessed November 27, 2002).

Ehlers, M., Welch, R., 1987. Stereocorrelation of landsat TM images. Photogrammetric Engineering and Remote Sensing 53 (9), 1231–1237.

Farr, T.G., Hensley, S., Rodriguez, E., Martin, J., Kobrick, M., 2000. The shuttle radar topography mission. Proceedings of the CEOS SAR Workshop, 26–29 October 1999. ESA SP-450, CNES, Toulouse, pp. 361–363.

Fujisada, H., 1994. Overview of ASTER instrument on EOS-AM1 platform. Proceedings of SPIE, vol. 2268. The International Society for Optical Engineering, pp. 14–36.

Fujisada, H., 1998. ASTER level 1 data processing algorithm. IEEE Transactions on Geoscience and Remote Sensing 36 (4), 1101–1112.

Fujisada, H., Iwasaki, A., Hara, S., 2001. ASTER stereo system performance. Proceedings of SPIE, vol. 4540. The International Society for Optical Engineering, pp. 39–49.

Giles, P.T., Franklin, S.E., 1996. Comparison of derivative topographic surfaces of a DEM generated from stereoscopic SPOT images with field measurements. Photogrammetric Engineering and Remote Sensing 62 (10), 1165–1171.

Kok, A.L., Blais, J.A.R., Rangayyan, R.M., 1987. Filtering of digitally correlated Gestalt elevation data. Photogrammetric Engineering and Remote Sensing 53 (5), 535–538.

Lang, H., Welch, R., 1999. Algorithm Theoretical Basis Document for ASTER Digital Elevation Models, Version 3.0 Jet Propulsion Laboratory, Pasadena, CA. 69 pp.

Lang, H., Welch, R., Miyazaki, Y., Bailey, B., Kelly, G., 1996. The ASTER along-track stereo experiment—a potential source of global DEM data in the late 1990's. Proceedings of SPIE, vol. 2817. The International Society for Optical Engineering, pp. 95–97.

O'Neill, M.A., Dowman, I.J., 1993. A simulation study of the ASTER sensor using a versatile general purpose rigid sensor modelling system. International Journal of Remote Sensing 14 (3), 565–582.

Schwartz, C. R., 1989. North American Datum of 1983. Rockville, MD, NOAA Professional Paper NOS 2, National Geodetic Information Center, 256 pp.

Snyder, J.P. 1987. Map projections—a working manual. U. S Geological Survey Professional Paper 1395, 383 pp.

SPOT Image, 2001. SPOT 5: delivering the world in 3D. World Wide Web article appeared on Directions Magazine (9/26/2001 issue), URL: http://www.directionsmag.com/pressreleases.asp?PressID=3856 (accessed November 27, 2002).

Tokunaga, M., Hara, S., Miyazaki, Y., Kaku, M., 1996. Overview of DEM product generated by using ASTER data. International Archives of Photogrammetry and Remote Sensing 31 (B4), 874–878.

Topographic Science Working Group, 1988. Topographic Science Working Group report to the Land Processes Branch. Earth Science and Applications Division, NASA Headquarters: Lunar and Planetary Institute, Houston, TX, 64 pp.

Welch, R., 1985. Cartographic potential of SPOT image data. Photogrammetric Engineering and Remote Sensing 51 (8), 1085–1091.

Welch, R., 1990. 3-D terrain modeling for GIS applications. GIS World 3 (5), 26–30.

Welch, R., Marko, W., 1981. Cartographic potential of a spacecraft line array camera system: stereosat. Photogrammetric Engineering and Remote Sensing 47 (8), 1173–1185.

Welch, R., Jordan, T., Lang, H., Murakami, H., 1998. ASTER as a source for topographic data in the late 1990's. IEEE Transactions on Geoscience and Remote Sensing 36 (4), 1282–1289.

Yamaguchi, Y., Kahle, A.B., Tsu, H., Kawakami, T., Pniel, M., 1998. Overview of advanced spaceborne thermal emission and reflection radiometer (ASTER). IEEE Transactions on Geoscience and Remote Sensing 36 (4), 1062–1071.